A FUSION MEASUREMENT METHOD FOR NANO-DISPLACEMENT BASED ON KALMAN FILTER AND NEURAL NETWORK

Zhuoliang Zhang,*,** Chao Zhou,* Zhangming Du,*,** Lu Deng,*** Zhiqiang Cao,* Shuo Wang,* Long Cheng,* and Sai Deng*

Abstract

Nano-displacement measurement is one of the most important aspects of nanomanipulation. However, the narrow working space and the heat sensitivity of the microscope limit the installation of many displacement sensors. The self-sensing and time-digit-conversion (TDC) method can overcome the above limitations, making these two methods ideal for nano-displacement measurement. The former method has a high sampling frequency, but its accuracy is low. In contrast, the TDC method is more accurate, but its sampling rate is low. To solve these problems, a fusion measurement method was proposed, thus allowing us to combine the results of the self-sensing and TDC. Specifically, an improved Kalman filter was used to overcome the asynchronous multi-rate problem. Moreover, we fully utilized the information of the calibration instrument using the neural network. As for the overfitting problem, we adopted a neural network with convolution filtering. Our method achieved a precision of 47.9% higher than the traditional method, as well as a linearity (R^2) of 0.99990 throughout 3,500 nm range.

Key Words

Multi-rate fusion, state block, convolution filtering, nanoscale measurement

1. Introduction

Due to the wide application of nanotechnology, the research work on nanomanipulation has increased year by year. Researchers have proposed some nanomanipulation systems [1]–[4] as well as some tracking control methods [5]–[7]. Other research work realized the application of nanomanipulation in biology [8] and photonics [9]. To obtain the feedback of the control system in nanomanipulation, it is necessary to effectively measure the displacement of the actuator. Some nanoscale displacement sensors are commonly used in nanomanipulation, including laser interferometer, eddy-current sensor, capacitive sensor and resistance strain gauge. These sensors generally have the disadvantages of large heat generation and difficulty in installation. The former disadvantage limits the duration of continuous operation, while the latter limits the installation of the sensors in nanomanipulation platforms [10], [11]. For example, although laser interferometers have the advantages of high precision, they are bulky and expensive and require a complex auxiliary optical system. Therefore, it is difficult to integrate a laser interferometer into a nanomanipulation system, such as the chamber of a scanning electron microscope (SEM). In addition, laser interferometers emit heat during operation, which is hard to dissipate in SEM's vacuum chamber and causes thermal drifts. For the above reasons, laser interferometers are usually used as calibration instruments.

To improve the performance of the displacement measurement in microscope, researchers have proposed several new measurement methods for nanoscale displacement, including self-sensing and time-digit-conversion (TDC) [12], [13]. The former method does not require additional sensors, which eliminates mechanical errors caused by assembly. The latter method reduces heat generation. Both methods reduce the heat emitted to the workspace and are easy to install in the microscope. The accuracy of the self-sensing method is lower because of the drift of charge measurement. In contrast, the TDC method is more accurate, but its sampling rate is low due to time measurement. To combine the advantages of these two measurement methods, it is necessary to use data fusion technologies for fusion measurement.

Data fusion is a processing technology for multi-source data or information, mainly to obtain more accurate measured data through data association and combination. Especially in the field of robotics and control, researchers have developed many data fusion technologies to improve the feedback accuracy of control systems [14]–[17]. Because self-sensing and TDC have different rates and are

* State Key Laboratory of Management and Control for Complex Systems, Institute of Automation, Chinese Academy of Sciences, Beijing, China; e-mail: {zhangzhuoliang2018, chao.zhou, duzhangming2015, zhiqiang.cao, shuo.wang, long.cheng, dengsai2012}@ia.ac.cn

** School of Artificial Intelligence, University of Chinese Academy of Sciences, Beijing, China

*** School of Statistics and Mathematics, Central University of Finance and Economics, Beijing, China; e-mail: denglu521@sina.com

Corresponding author: Chao Zhou

Recommended by Prof. Maki K. Habib
(DOI: 10.2316/J.2021.206-0421)

asynchronous, this paper focused on the asynchronous multi-rate data fusion. The typical algorithms are the following: Alouani and Rice [18] considered observations in the same sampling period as synchronized and then used a distributed fusion structure with feedback for processing. Lin *et al.* [19] converted asynchronous sensor measurements into synchronized measurements with additional noise, and the final state estimates were biased. Hu *et al.* [20] proposed a fusion method for batch processing in terms of sampling period, which was based on discretization of continuous systems. A common disadvantage of the above methods is that they have poor real-time performance. Moreover, the above methods are model based, and the data of the high-precision instrument are only used for the calibration of a single sensor or to determine certain parameters in their models. The inadequate use of calibration instrument information reduces the accuracy of these methods.

In our previous work [21], a nanoscale displacement fusion measurement method was proposed. On this basis, this paper extended the Kalman filtering with state block to asynchronous systems. Aiming at the overfitting problem of neural network, this paper adopted a neural network with convolution filtering. Experiments showed that our algorithm has better performance in terms of accuracy, linearity, resolution and drift, as well as better real-time performance.

2. System Setup

The experimental system consisted of piezoelectric ceramics, drive circuit, self-sensing measurement circuit, TDC measurement circuit, laser interferometer, MCU and PC. All devices except the PC were mounted on a vibration isolation table. The voltage that drives the piezoelectric ceramic can be manually adjusted or controlled by the PC.

The self-sensing method added no detectors to the nanomanipulation platform but only connected a sensing circuit to the driver of actuator [13]. In the TDC method, a TDC processor and a half-bridge circuit were used as the measurement circuit [9]. The raw data were transmitted to the MCU through the serial peripheral interface (SPI) for pre-processing and then transferred to the PC for further processing. The TDC method was limited by the charge and discharge time of the capacitor, and its sampling frequency can only reach 24.4 Hz. The frequency of the self-sensing method was set to 10 times that of the TDC method, *i.e.* 244 Hz, although this frequency can be higher. In addition, a laser interferometer (SIOS SP2000 TR) with a resolution of 0.1 nm was used to provide the standard value for displacement. The experimental setup is shown in Fig. 1. The system hardware is shown in Fig. 2.

3. Data Fusion Method

To combine the advantages of self-sensing and TDC, a data fusion technology was used for fusion measurement. However, self-sensing and TDC have different rates and are asynchronous, which cannot be fused by traditional single-rate synchronous methods. So, in this paper, the

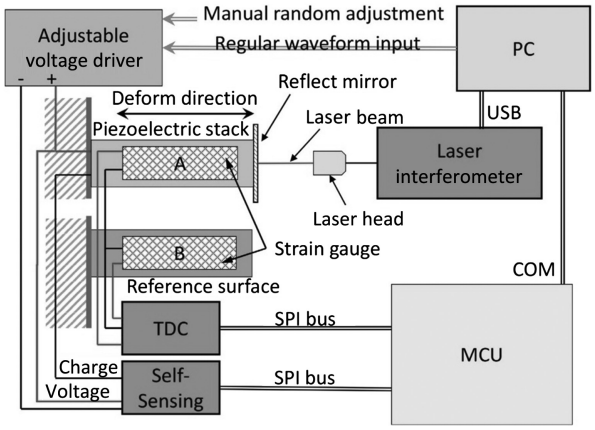

Figure 1. Experimental setup.

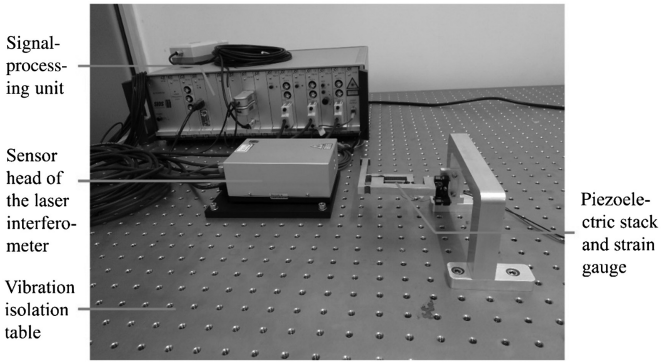

Figure 2. System hardware.

Kalman filter was used to transform the asynchronous multi-rate problem into a synchronous single-rate one. In this method, the state space was divided according to the sampling rate of each sensor, and then the adaptive Kalman filter was used to process the system, and finally the single-rate estimations were obtained. This bundling strategy allows asynchronousness to occur only within the state blocks. As long as we divide the state space of each sensor synchronously, the synchronization of the block system can be guaranteed. In addition, we divided the state space into blocks with a sliding window so that the system can work in real time. After obtaining the synchronous single-rate estimated value, we used the neural network as the fusion method, making full use of the data of the calibration instrument, thus improving the accuracy of the fusion measurement. To solve the overfitting problem of the network, we also adopted a neural network with convolution filtering. This network can learn filters from the data, which reduces the noise of the data. As a result, the possibility of the network getting overfitting can be reduced. The flow chart of our method is shown in Fig. 3.

3.1 Kalman Filter with Improved State Block

We defined the rates of the asynchronous multi-rate sensors as S_1, $S_2 \cdots, S_N$, and $S_1 \leq S_2 \leq \cdots \leq S_N$. Assume

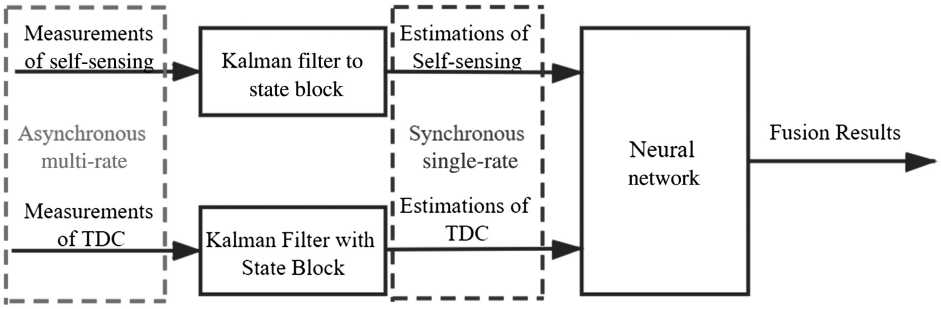

Figure 3. Flow chart of the proposed method with Kalman filter and neural network.

that the sampling rate of two adjacent sensors satisfies the integer multiple relationship:

$$S_{i+1} = n_i * S_i, \qquad i = 1, 2, \cdots, N-1 \tag{1}$$

And $n_0 \triangleq 1$. Based on the above basic definition, an asynchronous multi-rate sensor system can be described as [22]:

$$x(N, k+1) = A(N,k)x(N,k) + w(N,k) \tag{2}$$
$$z(i,k) = H(i,k)x(i,k) + v(i,k), \quad i = 1, 2, \cdots, N \tag{3}$$

where $x(N,k) \in \mathbb{R}^n$ is the system state of the rate S_N. $z(i,k) \in \mathbb{R}^{q_i} (q_i \leq n)$ is the observation of the ith sensor with a rate of S_i. $x(i,k)$ is the smoothest information of the state $x(N,\cdot)$ at the kth observation time of the sensor i and is determined as below:

$$x(i,k) = \frac{1}{\tilde{M}_i} \sum_{l=0}^{\tilde{M}_i - 1} x(N, \tilde{M}_i k - l)$$
$$\tilde{M}_i = \begin{cases} \prod_{j=i}^{N-1} n_j, & i = 1, 2, \cdots, N-1 \\ 1, & i = N \end{cases} \tag{4}$$

The process error $w(N,k) \in \mathbb{R}^{n \times 1}$ and the observation error $v(i,k) \in \mathbb{R}^{q_i \times 1}$ are white noise sequences and are uncorrelated. Define $M_i = \prod_{j=0}^{i-1} n_j$, $M = M_N$, then the original linear system (2) and (3) can be rewritten as:

$$X_N(k+1) = A_N(k)X_N(k) + W_N(k) \tag{5}$$
$$Z_i(k) = H_i(k)X_N(k) + V_i k) \tag{6}$$

where

$$X_N(k) = \begin{bmatrix} x(N,(k-1)M+1) \\ x(N,(k-1)M+2) \\ \vdots \\ x(N,kM) \end{bmatrix} \tag{7}$$

$$H_i(k) = \frac{1}{\tilde{M}_i} diag\{H(i,(k-1)M_i+1)I_{\tilde{M}_i}, H(i,(k-1)M_i+2)I_{\tilde{M}_i}, \cdots, H(i,kM_i)I_{\tilde{M}_i}\} \tag{8}$$

$$A_N(k) = \begin{bmatrix} 0 & 0 & \cdots & A(N,kM) \\ 0 & 0 & \cdots & A(N,kM+1)A(N,kM) \\ \vdots & & \ddots & \vdots \\ 0 & 0 & \cdots & \prod_{l=M-1}^{0} A(N,kM+l) \end{bmatrix} \tag{9}$$

$$Z_i(k) = \begin{bmatrix} z(i,(k-1)M_i+1) \\ z(i,(k-1)M_i+2) \\ \vdots \\ z(i,kM_i) \end{bmatrix} \tag{10}$$

Here $I_{\tilde{M}_i} = [\, I_n \; I_n \; \cdots \; I_n \,]$ is composed of $\tilde{M}_i$ unit matrices with n dimensions. $W_N(k)$ and $V_i(k)$ are uncorrelated with each other and are white noise sequences that satisfy a normal distribution [22].

N models can be obtained through the above method, then the optimal state estimates can be obtained using the classical Kalman filter for each of the N models. As these models will output M estimates for each block, the multi-rate problem is converted into a single-rate problem. The state blocks were divided synchronously in the original asynchronous system, making asynchronous only appear inside the blocks.

For the single-rate output after Kalman filtering, Yan *et al.* [22] proposed an unbiased fusion estimation. However, this method has poor real-time performance and requires prior information [21]. Because this method treats the measured value in each state block as a whole, when the observer needs to know the estimated value at a certain moment, he must wait until all the measured values corresponding to the current state block are obtained. From the perspective of the observer, the fusion algorithm seems to output the estimations "piece by piece". The actual output frequency is S_N/M, which is much lower than the highest sampling rate (S_N) in the system.

To overcome the lack of real-time performance, the original state block method was improved with a sliding window. As the state blocks span M in time, M different block methods will be generated when the block method is slid on the time axis, as shown in Fig. 4. This ensures that there exists a block method at any time, in which the measured values in the corresponding state block are all known. For example, the red box in Fig. 4 is block method 1, and the blue box is block method 2. The fusion

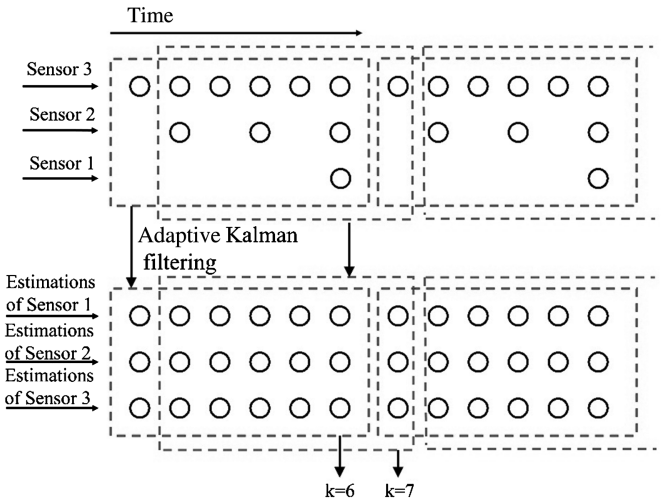

Figure 4. Kalman filter with improved state block.

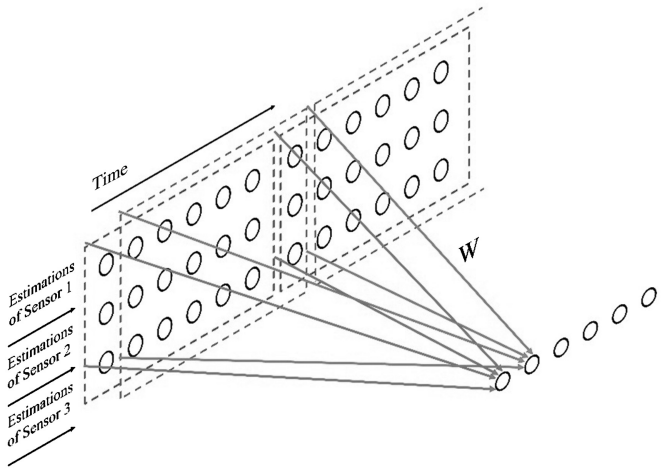

Figure 5. Convolutional filter sliding on time axis.

estimation when $k = 6$ is obtained by method 1, and the fusion estimation when $k = 7$ is obtained by method 2. The output frequency of the sliding window state block method is S_N, which is M times that of the method in [22], so our method has better real-time performance.

To improve the robustness of the method, the traditional Kalman filter was replaced by adaptive Kalman filter. The matrices Q and R were automatically modified during the measurement:

$$Q_{k+1} = \frac{1}{k+1}(kQ_k + K_{k+1}v_{k+1}v_{k+1}^T K_{k+1}^T + P_{k+1}) \quad (11)$$

$$R_{k+1} = \frac{1}{k+1}(kR_k + v_{k+1}v_{k+1}^T) \quad (12)$$

It can be proved that the algorithm can guarantee the convergence of the filter [23].

3.2 Neural Network with Convolution Filtering

The neural network was adopted to improve the accuracy of the fusion measurement. Under the experimental conditions of this paper, the neural network tended to fit the noise due to the large noise contained in the data set. As a result, the network was extremely vulnerable to overfitting [24]. Existing methods for preventing overfitting include early stop [25], regularization and dropout [26]. However, none of these methods directly deal with the noise itself. In actual tests, such methods did not perform well in the case of large noise. Therefore, we referred to the design method of convolutional neural network (CNN), using a neural network with convolution filtering to solve the overfitting problem.

A typical CNN consists of some layers with specific functions [27]. The convolutional layer implements the operation of CNN to reduce overfitting, *i.e.*, convolution filtering. The convolutional layer enables the network to learn the filter from the data, thus directly reducing the noise of the data. Moreover, the convolution filter possesses the properties of local connection and parameter sharing, which reduces the number of training parameters and the possibility of overfitting.

We expanded the state estimate of the improved Kalman filter on the time axis and slid the convolution kernel on the time axis as shown in Fig. 5. The length of the convolution kernel was set to be equal to the length of the data block (*i.e.* M), so that the adoption of convolution filtering did not reduce the real-time performance of the entire system.

In practical applications, only the current measurement and some previous measurement values can be known, so it was impossible to add more layers after the convolution layer, such as the pooling layer or the second convolution. This results in a failure to fit the non-linear mapping. Therefore, we replaced the convolution filter with a back propagation (BP) neural network. When the BP neural network slides on the time axis, the first layer of the network has the function of a convolution filter, while maintaining the non-linear mapping ability of the entire network. From the time axis, the network also satisfies the properties of local connections and parameter sharing, suppressing the occurrence of overfitting. The input and output structure of the neural network were determined in the same way as our previous work [21].

4. Experiments

In this section, the measured displacement was set to specific waveforms, and the performance of the relevant methods was tested.

4.1 Results of the Displacement Measurement

Firstly, a random waveform voltage was applied to the piezoelectric ceramics. The measurement results are shown in Fig. 6. The local enlargement presents that when both self-sensing and TDC deviated from the interferometer result, the fusion result of our method was still close to the interferometer. The performance of various measurement methods was calculated as shown in Table 1. In this table, the best values for each row are depicted in bold typeface. Our method can achieve higher precision and an output frequency equal to the self-sensing method.

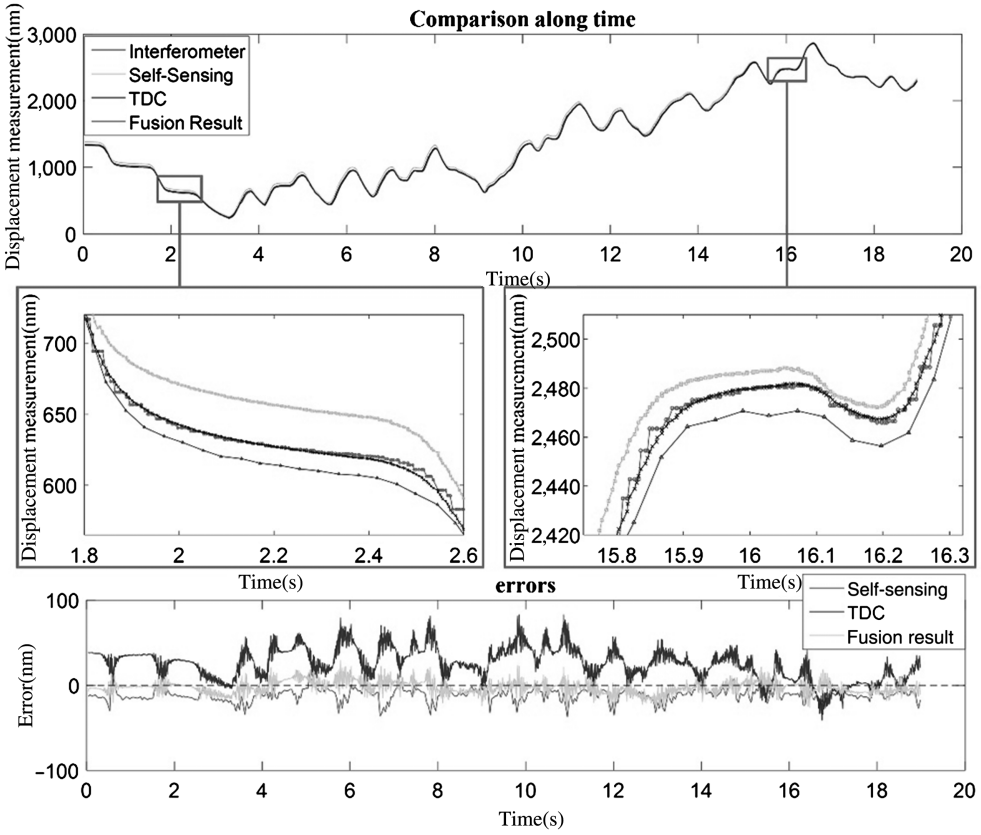

Figure 6. Measurement results of random signal, local enlargements and error curves.

Table 1
Measurement Performance (Randomly Adjusted Displacement)

Performance	Methods			
	Self-sensing	TDC	Method in [22]	**Our method**
Linearity R^2	0.99945	0.99984	0.99959	**0.99990**
Average error	26.8859 nm	11.7136 nm	11.6031 nm	**6.0457 nm**
Root mean squared error (RMSE)	31.2975 nm	13.6396 nm	14.6801 nm	**7.6439 nm**
Resolution (6σ)	**0.8364 nm**	7.4089 nm	3.1154 nm	1.0394 nm
Sampling rate	244 Hz	24.4 Hz	24.4 Hz	**244 Hz**
Drift rate	0.9688 nm/s	0.2903 nm/s	0.5255 nm/s	**0.0431 nm/s**

4.2 Linearity

In this paper, the coefficient of determination (R^2) was used to measure the linearity of the displacement measurement. The linearity of our method was calculated to be 0.99990, which was the highest among the relevant methods. Linearity-related data are listed in Table 1.

We also tested the performance of the fusion method for higher frequency signals. A modulated sinusoidal voltage was applied to the piezoelectric ceramic with a carrier frequency of 1.6 Hz, and the measurement results are shown in Fig. 7. As the signal changed at a higher frequency, the time lag effect between sampling of each method and interferometer was amplified, thus increasing the errors. The relevant data are listed in Table 2. In this table, the best values for each row are depicted in bold typeface. At this time, the fusion method also achieved superior performance, which was significantly better than the method in [19].

4.3 Resolution

In this paper, the 6σ-resolution proposed in [11] was used to measure the minimum distance of the measurement results. To visually display the noise of the measurement results, the voltage on the piezoelectric ceramic was raised from 0 to a fixed value (30 V) and remained constant for a certain period. According to [11], the resolution of our

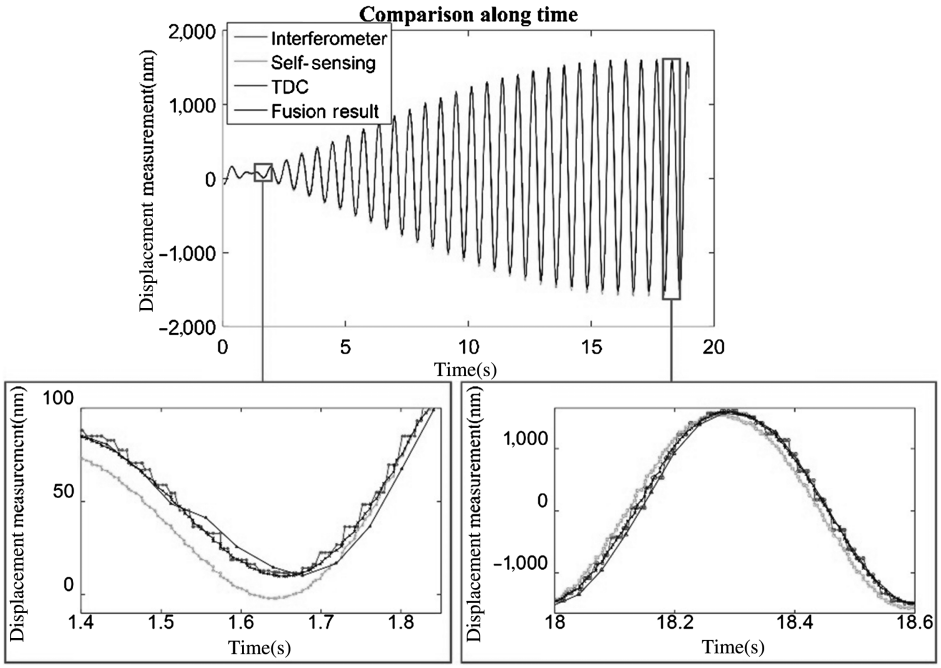

Figure 7. Measurement results of modulated sinusoidal signal and local enlargement.

Table 2
Measurement Performance (Modulated Sinusoidal Waveform with a Carrier Frequency of 1.6 Hz)

Performance	Methods			
	Self-sensing	TDC	Method in [22]	**Our method**
Linearity R^2	0.97899	0.98991	0.96990	**0.99600**
Average error	88.1521 nm	51.9318 nm	99.7673 nm	**33.8957 nm**
Root mean squared error (RMSE)	119.2866 nm	81.0760 nm	139.6916 nm	**50.8115 nm**
Sampling rate	244 Hz	24.4 Hz	24.4 Hz	**244 Hz**

method was 1.0394 nm. The comparison of resolutions is shown in Table 1.

4.4 Drift

To compare the drift of different measurement methods, we increased the voltage on the piezoelectric ceramic from 0 to a fixed value (7 V) and continued to measure for a certain period. The measurement results are shown in Fig. 8. The straight line was used to fit the measurement results from 60 s to 150 s, and the slope of the line was used to measure the drift rates of the related methods. The fitting results are shown in Fig. 9. The drift rate of our method was 0.0431 nm/s, which was the lowest among the relevant methods.

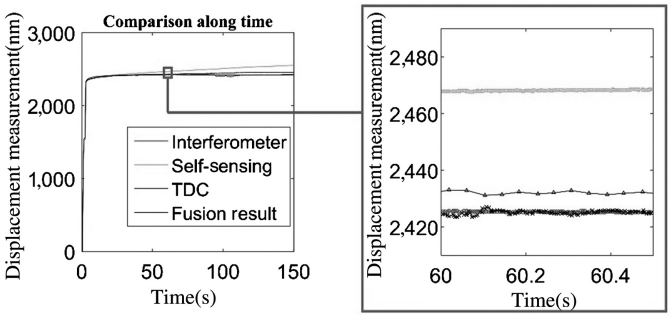

Figure 8. Results of fixed displacement and local enlargement.

5. Conclusion

In this paper, a novel nanoscale displacement fusion measurement method for self-sensing and TDC was proposed. In this method, the state space was divided according to the sampling rate of each sensor, and then the adaptive Kalman filter was used to process the blocked system, and finally the single-rate estimated value was obtained. This bundling strategy allows asynchronousness to occur only within the state blocks. Moreover, we used the neural network with convolution filtering as the fusion method. Our method achieved a linearity (R^2) of 0.99990 throughout 3,500 nm range, as well as 6σ-resolution of 1.0394 nm. More importantly, our method reduced the heat emitted to the workspace and was easy to install in the microscope. Our method was also a more economical method; its price ($600) was only 2% of the price of the laser in-

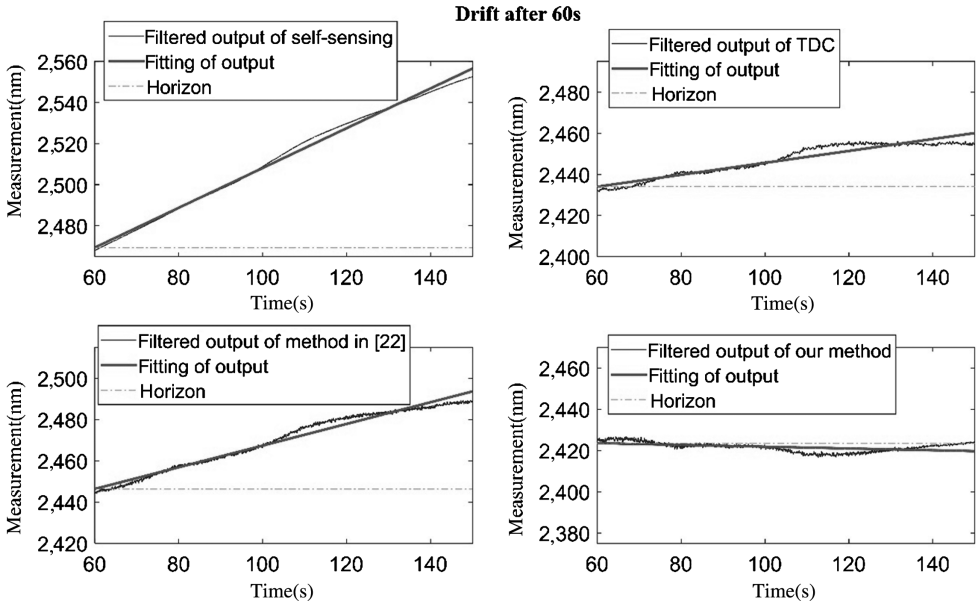

Figure 9. Comparison of drift rates after 60 s.

terferometer ($30,000). The next step can be using our method for actual nanomanipulation tasks. In addition, our algorithm is a universal asynchronous multi-rate fusion method that can be widely used in environmental monitoring, resource management, geological analysis, urban planning and large-scale economic information systems. In the future, we can study the application of this method in the control of complex industrial processes, such as identifying system failures and triggering alarms. We can also study the application in robot control, using the redundancy and complementarity of sensors to obtain more accurate environmental information, thus improving the control performance of intelligent robots.

Acknowledgement

This work was supported by the National Natural Science Foundation of China (Grant No. 61903362, Grant No. 62033013) and the National Social Science Fund of China (Grant No. 20BTJ042).

References

[1] D. Lixin, F. Arai, and T. Fukuda, Destructive constructions of nanostructures with carbon nanotubes through nanorobotic manipulation, *IEEE/ASME Transactions on Mechatronics, 9*(2), 2004, 350–357.

[2] S. Fatikow, T. Wich, H. Hulsen, T. Sievers, and M. Jahnisch, Microrobot system for automatic nanohandling inside a scanning electron microscope, *IEEE/ASME Transactions on Mechatronics, 12*(3), 2007, 244–252.

[3] D. Zhang, J. Breguet, R. Clavel, V. Sivakov, S. Christiansen, and J. Michler, In situ electron microscopy mechanical testing of silicon nanowires using electrostatically actuated tensile stages, *Journal of Microelectromechanical Systems, 19*(3), 2010, 663–674.

[4] J. Wang and S. Guo, Development of a precision parallel micromechanism for nano tele-operation, *International Journal of Robotics and Automation, 23*(1), 2008, 56–63.

[5] H. Zhang, Z. Wang, H. Yan, F. Yang, and X. Zhou, Adaptive event-triggered transmission scheme and H_∞ filtering codesign over a filtering network with switching topology, *IEEE Transactions on Cybernetics, 49*(12), 2019, 4296–4307.

[6] H. Yan, P. Li, H. Zhang, X. Zhan and F. Yang, Event-triggered distributed fusion estimation of networked multisensor systems with limited information, *IEEE Transactions on Systems, Man, and Cybernetics: Systems, 50*(12), 2020, 5330–5337.

[7] H. Yan, H. Zhang, F. Yang, C. Huang, and S. Chen, Distributed H_∞ filtering for switched repeated scalar nonlinear systems with randomly occurred sensor nonlinearities and asynchronous switching, *IEEE Transactions on Systems, Man, and Cybernetics: Systems, 48*(12), 2018, 2263–2270.

[8] Z. Gong, B.K. Chen, J. Liu, C. Zhou, D. Anchel, X. Li, J. Ge, D.P. Bazett-Jones, and Y. Sun, Fluorescence and SEM correlative microscopy for nanomanipulation of subcellular structures, *Light: Science & Applications, 3*, 2014, e224.

[9] H.-Y. Chen, C.-L. He, C.-Y. Wang, M.-H. Lin, D. Mitsui, M. Eguchi, T. Teranishi, and S. Gwo, Far-field optical imaging of a linear array of coupled gold nanocubes: Direct visualization of dark plasmon propagating modes, *ACS Nano, 5*(10), 2011, 8223–8229.

[10] C. Zhou, Z. Gong, B.K. Chen, Z. Cao, J. Yu, C. Ru, M. Tan, S. Xie, and Y. Sun, A closed-loop controlled nanomanipulation system for probing nanostructures inside scanning electron microscopes, *IEEE/ASME Transactions on Mechatronics, 21*(3), 2016, 1233–1241.

[11] A.J. Fleming, A review of nanometer resolution position sensors: Operation and performance, *Sensors and Actuators A: Physical, 190*, 2013, 106–126.

[12] C. Zhou, Y. Wang, L. Deng, Z. Wu, Z. Cao, S. Wang, and M. Tan, A TDC-based nano-scale displacement measure method inside scanning electron microscopes, *2016 IEEE International Conf. on Robotics and Biomimetics (ROBIO)*, Qingdao, China, 2016, 1298–1302.

[13] Z. Du, T. Zhang, L. Deng, C. Zhou, Z. Cao, and S. Wang, A charge-amplifier based self-sensing method for measurement of piezoelectric displacement, *2017 IEEE International Conf. on Mechatronics and Automation (ICMA)*, Takamatsu, Japan, 2017, 1995–1999.

[14] N.-V. Nguyen, G. Shevlyakov, and V. Shin, Fusion of correlated local estimates under non-gaussian channel noise, *International Journal of Robotics and Automation, 25*(2), 2010, 155–161.

[15] S. Saeedi, L. Paull, M. Trentini, and H. Li, Occupancy grid map merging for multiple robot simultaneous localization and mapping, *International Journal of Robotics and Automation, 30*(2), 2015, 149–157.

[16] Z.W. Wang, Q.X. Cao, N. Luan, and L. Zhang, A novel autonomous localization technique of subsea in-pipe robot, *International Journal of Robotics and Automation, 25*(2), 2010, 102–108.

[17] M. Perrollaz, R. Labayrade, D. Gruyer, A. Lambert, and D. Aubert, Proposition of generic validation criteria using stereo-vision for on-road obstacle detection, *International Journal of Robotics and Automation, 29*(1), 2014, 32–43.

[18] A.T. Alouani and T.R. Rice, On optimal synchronous and asynchronous track fusion, *Optical Engineering, 37*(2), 1998, 427–433.

[19] X. Lin, Y. Bar-Shalom, and T. Kirubarajan, Multisensor multitarget bias estimation for general asynchronous sensors, *IEEE Transactions on Aerospace & Electronic Systems, 41*(3), 2005, 899–921.

[20] Y. Hu, Z. Duan, and C. Han, Optimal batch asynchronous fusion algorithm, *IEEE International Conf. on Vehicular Electronics & Safety*, Shann'xi, China, 2005, 237–240.

[21] Z. Zhang, Z. Du, L. Deng, C. Zhou, Z. Cao, S. Wang, and L. Cheng, A fusion measurement method based on Kalman filter with improved state block and neural network for nanometer displacement, *2018 IEEE International Conf. on Mechatronics and Automation (ICMA)*, Changchun, China, 2018, 539–544.

[22] L.P. Yan, B.S. Liu, and D.H. Zhou, The modeling and estimation of asynchronous multirate multisensor dynamic systems, *Aerospace Science & Technology, 10*(1), 2006, 63–71.

[23] C. Price, An analysis of the divergence problem in the Kalman filter, *IEEE Transactions on Automatic Control, 13*(6), 1968, 699–702.

[24] L. Yu, S. Wang, and K.K. Lai, An integrated data preparation scheme for neural network data analysis, *IEEE Transactions on Knowledge & Data Engineering, 18*(2), 2005, 217–230.

[25] X.X. Wu and J.G. Liu, A new early stopping algorithm for improving neural network generalization, *International Conf. on Intelligent Computation Technology & Automation*, Changsha, Hunan, China, 2009, 15–18.

[26] E. Phaisangittisagul, An analysis of the regularization between L2 and dropout in single hidden layer neural network, *International Conf. on Intelligent Systems*, Bangkok, Thailand, 2016, 174–179.

[27] Y. Lecun, L. Bottou, Y. Bengio, and P. Haffner, Gradient-based learning applied to document recognition, *Proceedings of the IEEE, 86*(11), 1998, 2278–2324.

Biographies

Zhuoliang Zhang received the B.E. degree in automation from Tongji University, Shanghai, China, in July 2018. He is currently pursuing the joint Ph.D. degree in control theory and control engineering with the Institute of Automation, Chinese Academy of Sciences and also with the University of Chinese Academy of Sciences, Beijing. His research interests include measurements, sensor signal processing and intelligent control.

Chao Zhou received the B.S. degree (Hons.) in automation from Southeast University, Nanjing, China, in July 2003, and the Ph.D. degree in control theory and control engineering from the Institute of Automation, Chinese Academy of Sciences, Beijing, China, in 2008. Since July 2008, he has been an assistant professor in the Key Laboratory of Complex Systems and Intelligent Science, Institute of Automation, Chinese Academy of Sciences, where he has been an associate professor since October 2011 and full professor since October 2016. His current research interests include the motion control of robot, the bio-inspired robotic fish and embedded system of robot.

Zhangming Du received the B.E. degree in control theory and control engineering from Zhejiang University, Hangzhou, China, in July 2015. He is currently working towards the Ph.D. degree in control theory and control engineering at the Institute of Automation, Chinese Academy of Sciences, Beijing. His research interests include measurements, intelligent control and nano/microrobots.

Lu Deng received the B.S. degree (in International Economics and Trade in 2003) and MA. Sc degree (in Econometrics in 2006) from Hebei University of Technology, Tianjin, China, and the Ph.D. degree in Econometrics from Nankai University, Tianjin, China, in 2009. She is currently a full professor with School of Statistics and Mathematics, Central University of Finance and Economics, China. Her current research interests include applied statistics, econometric modelling and extreme value theory.

Zhiqiang Cao received the B.S. and M.S. degrees from Shandong University of Technology, Jinan, China, in 1996 and 1999, respectively. In 2002, he received the Ph.D. degree in control theory and control engineering from the Institute of Automation, Chinese Academy of Sciences, Beijing, China. He is currently a professor in the State Key Laboratory of Management and Control for Complex Systems, Institute of Automation, Chinese Academy of Sciences. His research interests include service robot, intelligent control and multi-robot coordination.

Shuo Wang received the B.E. degree in electrical engineering from Shenyang Architecture and Civil Engineering Institute, Shenyang, China, in 1995, the M.E. degree in industrial automation from Northeastern University, Shenyang, China, in 1998, and the Ph.D. degree in control theory and control engineering from the Institute of Automation, Chinese Academy of Sciences, Beijing, China, in 2001. He is currently a professor with the State Key Laboratory of Management and Control for Complex Systems, Institute of Automation, Chinese Academy of Sciences. His research interests include robot learning, biomimetic robot, UVMS and multirobot systems.

Long Cheng received the B.S. (Hons.) degree in control engineering from Nankai University, Tianjin, China, in 2004, and the Ph.D. (Hons.) degree in control theory and control engineering from the Institute of Automation, Chinese Academy of Sciences, Beijing, China, in 2009. He is currently a full professor with the Institute of Automation, Chinese Academy of Sciences. He is also an adjunct professor with University of Chinese Academy of Sciences. He is currently serving as an Associate Editor/Editorial Board Member of IEEE Transactions on Cybernetics, Neural Processing Letters, Neurocomputing, International Journal of Systems Science and Acta Automatica Sinica. His current research interests include the rehabilitation robot, intelligent control and neural networks.

Sai Deng received the B.E. degree in automation from Xiangtan University, Hunan, China, in 2012, and the Ph.D. degree in control theory and control engineering from the Institute of Automation, Chinese Academy of Sciences (IACAS), Beijing, China, in 2018. He is currently an associate professor at IACAS, Beijing, China. His research interests include motion control of the robot and system fault diagnosis.